Monatshefte für Chemie 137, 717–735 (2006)
DOI 10.1007/s00706-005-0470-0

Monatshefte für Chemie
Chemical Monthly
Printed in Austria

Potentiometric and Multinuclear Magnetic Resonance Study of the Solution Equilibria Between Aluminium(III) Ion and *L*-Aspartic Acid

Predrag Djurdjević[1,*], **Ratomir Jelić**[1], **Ljubinka Joksović**[1], and **Mirjana Cvijović**[2]

[1] Faculty of Science, Chemistry Department, Kragujevac
[2] The Copper Mill, Sevojno-Uzice, State Union of Serbia and Montenegro (former Yugoslavia)

Received July 19, 2005; accepted (revised) September 5, 2005
Published online May 5, 2006

Summary. Solution equilibria between aluminium(III) ion and *L*-aspartic acid were studied by potentiometric, ^{27}Al, ^{13}C, and ^{1}H NMR measurements. Glass electrode equilibrium potentiometric studies were performed on solutions with ligand to metal concentration ratios 1:1, 3:1, and 5:1 with the total metal concentration ranging from 0.5 to 5.0 mmol/dm^3 in 0.1 mol/dm^3 LiCl ionic medium, at 298 K. The *pH* of the solutions was varied from *ca.* 2.0 to 5.0. The non-linear least squares treatment of the data performed with the aid of the Hyperquad program, indicated the formation of the following complexes with the respective stability constants log $\beta_{p,q,r}$ given in parenthesis (p, q, r are stoichiometric indices for metal, ligand, and proton, respectively): Al(H*Asp*)$^{2+}$ ($\log \beta_{1,1,1} = 11.90 \pm 0.02$); Al(*Asp*)$^{+}$ ($\log \beta_{1,1,0} = 7.90 \pm 0.03$); Al(OH)*Asp*^{0} ($\log \beta_{1,1,-1} = 3.32 \pm 0.04$); Al(OH)$_2$*Asp*$^{-}$ ($\log \beta_{1,1-2} = -1.74 \pm 0.08$), and Al$_2$(OH)*Asp*$^{3+}$ ($\log \beta_{2,1,-1} = 6.30 \pm 0.04$). ^{27}Al NMR spectra of Al^{3+} + aspartic acid solutions (*pH* 3.85) indicate that sharp symmetric resonance at $\delta \sim 10$ ppm can be assigned to $(1, 1, 0)$ complex. This resonance increases in intensity and slightly broadens upon further increasing the *pH*. In Al(*Asp*)$^{+}$ complex the aspartate is bound tridentately to aluminum. The ^{1}H and ^{13}C NMR spectra of aluminium + aspartic acid solutions at *pH* 2.5 and 3.0 indicate that β-methylene group undergoes the most pronounced changes upon coordination of aluminum as well as α-carboxylate group in ^{13}C NMR spectrum. Thus, in Al(H*Asp*)$^{2+}$ which is the main complex in this *pH* interval the aspartic acid acts as a bidentate ligand with –COO^{-} and –NH$_2$ donors closing a five-membered ring.

Keywords. Aluminium; Aspartic acid; Complex formation; Potentiometry; Multinuclear NMR.

Introduction

Aluminum can be regarded as detrimental and toxic element. The environment, the diet, or medication are the main sources of aluminum that enters human body. The

* Corresponding author. E-mail: preki@knez.kg.ac.yu

main sources of iatrogenic aluminum are now aluminum-containing phosphate binders and aluminum-containing antacids administered to uremic patients or those with gastric or duodenal ulcer. Among compounds of this class pharmaceutical formulations containing $AlPO_4$ or $Al(OH)_3$ have found widespread use. With normal renal and gi function endogenous aluminum is readily excreted in the urine and feces. Thus, physiological serum levels of aluminum are 0.07 to 0.3 μmol/dm^3. However, high tissue load of aluminum may be found in patients with chronic renal failure who are treated by dialysis fluids that contain aluminum, or are given Al-hydroxide gels to control high plasma level phosphate. Increased content of aluminum may also appear in patients taking large quantities of Al-based antacids. Patients with high tissue and serum level of aluminum may develop blood, bone, or brain diseases which may be linked to the excess of aluminum [1–3].

Because Al^{3+} is a hard metal ion it forms complexes of the highest stability with ligands containing hard donor groups. The most effective are the ligands possessing strongly basic negatively charged oxygen atoms (phenolates, alcoxides, carboxylates, phosphonates, *etc.*) and nitrogen atoms which are appropriately arranged to form five- or six-membered metalacycles (aminocarboxylates) [4]. Important biological molecules, proteins, peptides and amino acids contain electron-pair donor functional groups which can bind acceptor metal ions. These interactions are essential for metalloproteins and metalloenzymes but in case of aluminum they interfere or even block essential biological processes [5]. Although amino group plays a significant role in metal chelation, it does not bind Al^{3+} strongly except as part of multidentate systems involving other strong binding donors [6].

The amino acids which are the block units for the protein and peptide chain have amino and carboxylate groups able to bind metal ions. Though amino acids generally do not form strong complexes with aluminum ion, those with effective side chain donors (glutamic, aspartic) can form chelates of appreciable stability with Al^{3+} ion on account of favorable steric arrangement of donor groups [7, 8]. The stability of these chelates increases as the number and basicity of the donor groups increase. Aliphatic amino acids with non-polar side chain like glycine, alanine, leucine, *etc.*, are weak binders of aluminum owing to low basicity of their carboxylate group (pK_a 2–3). Methionine, cysteine, cystine, and lysine also exhibit weak binding due to low affinity of aluminum for sulfhydryl and amino groups [1]. Amino acids with polar side chain like glutamic and aspartic, containing two carboxylate and one central amino group are significantly stronger aluminum binders [9, 10]. The stability of the 1:1 complex is about two orders of magnitude higher than that of any simple glycine-like amino acid. This indicates involvement of both carboxylate groups in aluminum binding. Aspartic acid acts as a tridentate ligand with the formation of five- + six-membered chelates with aluminum ion [11]. In aspartate where the amino group is adjacent to two carboxylates which are strong aluminum binders, metal ion induced deprotonation of $-NH_3^+$ group with subsequent coordination of amino group is likely to occur. The tridentate coordinating ability of glutamate is much weaker due to the lower stability of the seven-membered chelate ring formed with participation of the terminal carboxylate group. Since however, 1:1 chelate of glutamate and aluminum ion shows enhanced stability $-NH_2$ involvement in coordination *via* the formation of five- + seven-membered rings was suggested by *Kiss et al.* [11].

L-Aspartic acid is a non-essential amino acid, synthesized from glutamate or derived from protein food. It is involved in building *DNA*, in carbohydrate metabolism, and protein metabolism. It is a carrier molecule for the transport of magnesium and potassium in cells. Aspartic acid is a major excitatory transmitter in brain. It not only acts as an excitatory neurotransmitter, but also participates in cerebral energy metabolism. Its concentration in brain tissue may be increased in patients with seizures and strokes [12]. Therapeutic amounts of aluminum may bind to aspartate and thus disrupt its metabolic pathways. Normal function of this amino acid may be thus, disturbed. In what extent such disturbance may occur, whether the Al-aspartate species are lipid soluble or not, can be answered if identity and stability of the complexes of Al with this amino acid are reliably determined.

Hence, understanding of the nature of aluminum–*L*-aspartate interactions would help to gain better insight in toxicity problems of aluminum. As already said, aspartate may bind aluminum ion either as monodentate, bidentate, or tridentate ligand. Monodentate binding mode involves the participation of carboxylate group only, bidentate mode may engage both the carboxylate and amino group while tridentate coordination implicates binding of carboxylate, amino group and carboxylate from side chain. The, side chain carboxylate is weakly acidic (pK_a in the range 4–5) and can serve as a site for aluminum complexation.

The objective of the present work was to study the complex formation between trivalent aluminum ion and *L*-aspartate with respect to speciation (identity and stability of the formed complexes) and binding mode of aspartate to aluminum. Review of available literature data shows that no unambiguous description of aluminum complexation with *L*-aspartic acid exists. *Duc et al.* [13] studied the complexation of aluminum with α-aminoacids that constitute the collagen by potentiometric measurements in $0.5\,\mathrm{mol/dm^3}$ $NaClO_4$ ionic medium at 298 K. With aspartate the complexes Al(OH)H*Asp*, $\beta = (9.4 \pm 0.4)\ 10^7$ and Al(H*Asp*), $\beta = (6.4 \pm 0.3)\ 10^{11}$ were found. *Kiss et al.* [11] have found the following complexation model (log β given in parenthesis): Al(H*Asp*), (11.76 ± 0.06), Al(*Asp*), (7.87 ± 0.04), Al*Asp*H_{-1} (3.30 ± 0.03), Al*Asp*H_{-2} (-2.32 ± 0.07) in $0.2\,\mathrm{mol/dm^3}$ KCl ionic medium at 25°C. No polynuclears were found owing to high ligand and ligand to metal concentration ratios. In the present work we studied the complex formation between aluminum ion and *L*-aspartic acid by glass electrode potentiometric measurements and ^{27}Al, ^{13}C, and ^{1}H NMR spectroscopy using lower total ligand concentration and ligand to metal concentration ratios from 1:1 to 5:1.

Results and Discussion

Protolytic Equilibria in Pure Aspartic Acid Solutions

Overall protonation constants, β_i of aspartate defined as Eq. (1), were determined from glass electrode potentiometric titration data of solutions of aspartic acid.

$$iH^+ + Asp^{2-} \rightleftharpoons HAsp^{(i-2)+}, \quad \beta_i \tag{1}$$

Three total concentrations of aspartic acid, 2.5, 5.0, and $10.0\,\mathrm{mmol/dm^3}$, were used. Appropriate amount of standard HCl was added in each solution. In total

Table 1. Summary of potentiometric data obtained in Al^{3+} – *Asp* system in 0.1 mol/dm^3 LiCl ionic medium at 298 K; all total concentrations, C_X, are in mmol/dm^3; the maximum attained average ligand number is denoted as Z_c; Npt is number of experimental points included in calculations

Entry	C_{Al}	C_{Asp}	C_H	*pH* interval	Npt	Z_c
1	5.0	15.0	35.0	2.378–5.041	53	1.78
2	5.0	25.0	55.1	2.466–4.811	41	2.67
3	2.5	7.5	20.1	2.373–4.783	36	2.14
4	2.5	12.5	30.1	2.434–4.960	54	2.95
5	1.0	3.0	11.1	2.344–4.839	55	2.08
6	1.0	5.0	15.1	2.393–4.800	61	1.80
7	0.5	1.5	8.05	2.335–4.827	52	1.13
8	0.5	2.5	10.1	2.330–4.820	56	1.35
9	4.8	5.0	15.4	3.519–4.521	21	0.80
10	2.5	3.0	11.3	3.489–4.250	20	0.89
11	–	2.5	5.0	2.340–9.593	60	–
12	–	5.0	15.3	1.885–10.53	70	–
13	–	10.0	17.2	1.920–10.08	70	–

200 points were collected. The constants were calculated with the aid of Hyperquad [14, 15] program. The obtained values $\log \beta_1 = 9.71 \pm 0.01$, $\log \beta_2 = 13.42 \pm 0.01$, $\log \beta_3 = 15.38 \pm 0.03$, are in good agreement with the literature data [11].

Equilibria in Aluminum(III) + Aspartic Acid Solutions

Potentiometric Measurements

A summary of the potentiometric experimental data is given in Table 1.

In the *pH* range studied (2.0–5.0) the maximum apparent ligand number reached was *ca.* 3.0. The highest concentration ratio of aspartate to Al^{3+} was 5:1. Beyond $pH = 5.2$, the solutions became turbid and drifting potential readings were obtained. No higher concentration ratios of aspartate to Al were used because they would seriously change the constancy of the medium. In addition, the buffering effect of aspartic acid may hinder the reliable potentiometric measurements. The establishing of equilibrium in solutions was moderately slow especially at the *pH* values higher than 4.0. High turbidity of solutions was observed at *pH* values near 5.5.

In order to derive the speciation model for the studied system the experimental data were plotted as the dependence of average ligand number, Z_{Al} on $-\log [Asp^{2-}]$.

Average ligand number of aluminium was calculated through Eq. (2) where C_X denotes total analytical concentration of the species X, while $[X]$ stands for equilibrium concentration of X.

$$Z_{Al} = \frac{C_{Asp} - [Asp]\{1 + \sum_i \beta_i [H^+]^i\}}{C_{Al}} \tag{2}$$

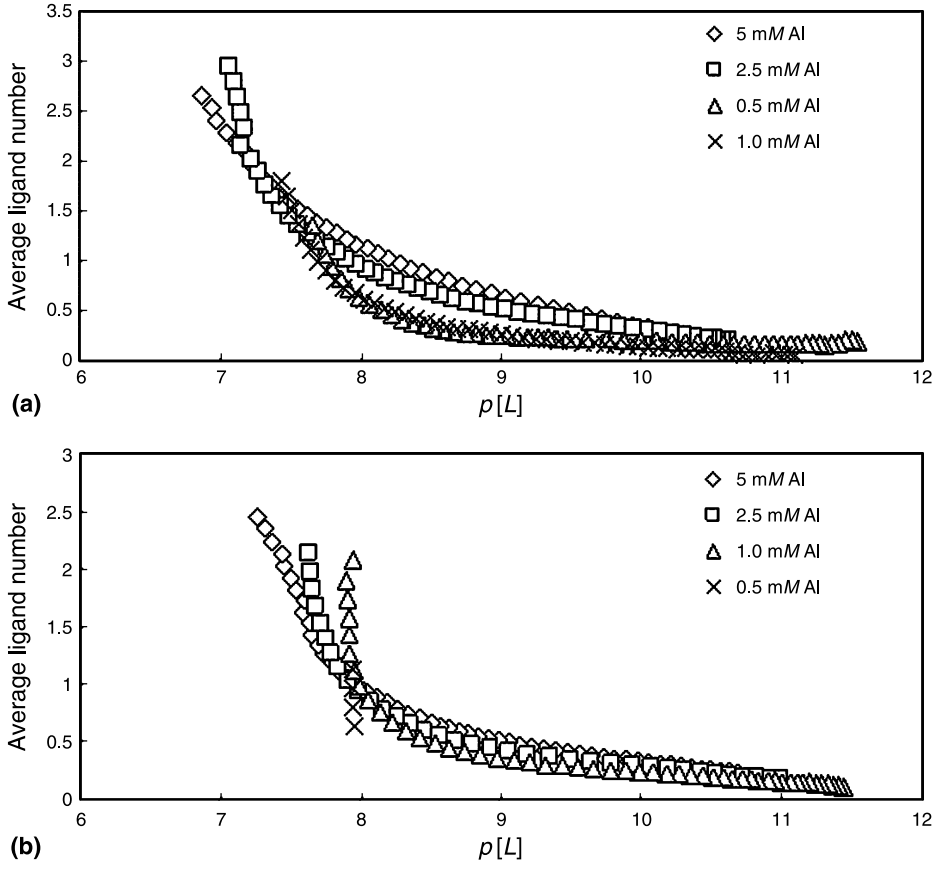

Fig. 1. Formation curves in $Al^{3+} + L$-aspartic acid solutions obtained by glass electrode potentiometric measurements at 298 K in 0.1 mol/dm^3 LiCl ionic medium; concentration ratio (a) 5:1 and (b) 3:1; $L = Asp^-$, $mM =$ mmol/dm^3

The equilibrium concentration of aspartate was calculated using Eq. (3) where symbols have their usual meaning.

$$[Asp] = \frac{C_H - [H^+] + [OH^-]}{\sum_i i\beta_i [H^+]^i} \tag{3}$$

Analysis of the formation curves (Fig. 1a and b) provides information that there are more species then simply Al(*Asp*) and/or Al(*Asp*)$_2$. For different C_{Al} and C_{Asp} the formation curves do not completely coincide; this is probably due to formation of protonated complexes (*e.g. ML*H, *ML*H$_2$, *etc.*). For $8.5 < p[Asp] < 11.0$ all formation curves superimpose. At $p[Asp] \sim 8.8$ curves begin to spread. This is where the concentration of protonated complexes maximizes. When Al(*Asp*) predominates the formation curves begin to superimpose once again. Further spreading is due to formation of mixed hydrolytic complexes. Values for average ligand number higher than 1 are obtained which indicates that protonated, the binary Al(*Asp*) complex, and mixed hydrolytic species are formed in parallel. To determine the composition and stability constants of the species formed, the titration data were analyzed using the program Hyperquad. The fit of the experimental data

was obtained by considering the following set of complexes: Al*L*H, Al*L*H$_2$, Al*L*(*L*H), Al(*L*H)$_2$, Al*L*, Al*L*$_2$, Al*L*H$_{-1}$, Al*L*H$_{-2}$, Al*L*$_2$H$_{-1}$, Al$_2$*L*H, Al$_2$*L*H$_{-1}$, Al$_2$*L*$_2$H$_{-2}$, Al$_2$*L*$_2$, Al$_2$*L*$_2$H$_{-1}$, Al$_2$*L* (*L* = *Asp*). In a first step a manual fitting option of Hyperquad was used. In Hyperquad calculations the identity and stability of complexes which give the best fit to the experimental data, were determined by minimizing the error-squares sum of the potentials, U (Eq. (4)), where w_i represents a statistical weight assigned to each point of the titration curve, E_{obs} and E_{calc} refer to the measured potential of the cell and the calculated one assuming the specific model and trial constants, respectively. The best model was chosen using the following criteria: (a) the lowest value of *U*; (b) standard deviation in calculated stability constants less than 0.15 log units; (c) standard deviations in potential residuals, defined as by Eq. (5) where *e* is a vector in potential residuals $(E_{obs} - E_{calc})$, *w* is a weighting matrix, *N* is the number of observations, and *k* is the number of refinable parameters, with standard deviation in volume readings 0.0005 cm^3 and standard deviation in potential readings 0.1 mV, should be less than 3.0; (d) goodness-of-fit statistics, χ^2 (*Pearson*'s test), at 95% confidence level, with 6 degrees of freedom, less than 12.6; and (e) reasonably random scatter of potential residuals without any significant systematic trends.

$$U = \sum w_i (E_{obs} - E_{calc})^2 \tag{4}$$

$$s = \{ewe^T/(N-k)\} \tag{5}$$

The titration curves were processed separately. The Hyperquad program provides very useful graphical analysis of the quality of fit. For each species introduced into the model the program calculates a simulated titration curve and speciation diagram thus showing the relative importance, *pH* region of formation, and influence on the overall fit of the chosen species. The stability constant is manually varied in small steps until best possible fit is achieved. This analysis proved that at higher aspartate to aluminum concentration ratios (5:1) the most important species are $(1,1,1)$ and $(1,1,0)$. Decreasing the concentration ratio of aspartate to aluminum the mononuclear mixed hydrolytic complexes become increasingly important. The species $(1,1,-1)$ and $(1,1,-2)$ appeared to give good coincidence between experimental and calculated titration curves. At concentration ratio of aspartate to aluminium 1:1 polynuclear species become dominant. We tried different polynuclears but acceptable agreement between experimental and calculated titration curves could only be achieved with the species $(2,1,-1)$. In this way most probable complexes were found and their trial stability constants were subjected to further Hyperquad refinement. The refinement operations for each aspartate to aluminum concentration ratio (L/M) resulted in different and often acceptable models. Different strategies were employed in the refinement operations: (i) fixing selected constants to simplify optimization procedure, (ii) reducing the number of experimental points included in calculations, (iii) parallel refinement of selected pure hydrolytic species together with the Al-*Asp* complexes, and (iv) ''piecewise'' fitting of the experimental data. The analytical parameters were always kept constant. The Hyperquad analysis showed that consistent formation constants for *ML*H and *ML* are always calculated with low standard deviations. The species *ML*H$_{-1}$ and *ML*H$_{-2}$ are normally accepted with $L/M = 5$ and $L/M = 3$, and corresponding

log β are obtained with acceptable standard deviation. All other mononuclear species from the above set of complexes did not give acceptable fit. During the calculation procedure in some tested models the complexes $(1,2,0)$ and $(2,2,0)$ with the stability constants $\log \beta_{1,2,0} = 14.91 \pm 0.12$ and $\log \beta_{2,2,0} = 19.52 \pm 0.13$ were accepted. Their inclusion in the model significantly worsened residual trends and unacceptable values for standard deviations in potential residuals were obtained. Thus, as the best model for the experimental data confined to $L/M = 5$ or 3, the *pH* region 2.5 to 5.0, and C_{Al} higher than $1.0\,\mathrm{mmol/dm^3}$, the set of complexes *ML*H, *ML*, *ML*H$_{-1}$, and *ML*H$_{-2}$ was derived. When the model consisting of *ML*H, *ML*, *ML*H$_{-1}$, and *ML*H$_{-2}$ complexes was established to fit the data with $C_{Al} \leq 1\,\mathrm{mmol/dm^3}$ and all the data with $L/M = 1$, we added various polynuclears from the initial set to this model fixing the values for *ML*H and *ML*. In all combinations only the complex $(2,1,-1)$ was accepted with improved statistical parameters. Introducing the $(2,1,-1)$ complex also resulted in rejection of $(1,1,2)$ complex which was temporarily accepted in some models. The complex $(2,2,0)$ found in Al – glutamate system [9] was always rejected. The complexes $(1,2,0)$ and $(2,1,-2)$ were tested in all models but in the competition with the afore mentioned set of complexes these were always rejected. No other stoichiometries were accepted in any of the calculations with the Hyperquad program. The best model for each ligand to metal concentration ratio is shown in Table 2.

Inspecting the data in Table 2 we conclude that only *ML*H, *ML*, *ML*H$_{-1}$, *ML*H$_{-2}$, and M_2LH$_{-1}$ form in significant amounts in the conditions used to record the titration curves at L/M concentration ratios ranging from 1:1 to 5:1. In final model selection we first optimized together all the data with $L/M = 5$ and $L/M = 3$. So obtained values of the stability constants were considered as definitive. We then separately re-calculated the data with $L/M = 1$ fixing the values of $(1,1,1)$ and $(1,1,0)$ complexes obtained in previous procedure and allowing the $(1,1,-1)$, $(1,1,-2)$, and $(2,1,-1)$ constants to float. The procedure resulted in rejection of $(1,1,-2)$ complex and very slight increase of the stability constant of $(2,1,-1)$ complex. In final model selection we choose mean value for the stability constant of the $(1,1,-2)$ complex. The finally selected model is given in Table 3. The

Table 2. Model optimization of Al^{3+} – aspartic acid complex formation in $0.1\,\mathrm{mol/dm^3}$ LiCl ionic medium at 25°C

Species (p,q,r)	$\log \beta_{p,q,r} \pm \sigma$		
	$L/M = 5$; $2.5 < pH < 5.0$	$L/M = 3$; $2.5 < pH < 4.8$	$L/M = 1$; $3.5 < pH < 4.5$
$(1,1,1)$	11.92 ± 0.02	11.88 ± 0.04	11.96 ± 0.07
$(1,1,0)$	7.81 ± 0.01	7.90 ± 0.05	–
$(1,1,-1)$	3.28 ± 0.02	3.38 ± 0.04	3.39 ± 0.04
$(1,1,-2)$	-1.70 ± 0.01	-1.73 ± 0.02	–
$(2,1,-1)$	6.28 ± 0.02	6.30 ± 0.04	6.35 ± 0.03
Statistical parameters of the fit	$\chi^2 = 12.27$; $s = 0.75$	$\chi^2 = 10.8$; $s = 1.47$	$\chi^2 = 13.0$; $s = 1.28$

Table 3. Selected values of the stability constants of aluminum – aspartate complexes

Complex	log $\beta_{p,q,r}$		
	This work	Ref. [11]	Ref. [16]
Al(H*Asp*)	11.90 ± 0.02	11.76 ± 0.06	11.24 ± 0.03
Al(*Asp*)	7.90 ± 0.03	7.87 ± 0.04	7.77 ± 0.02
Al(OH)*Asp*	3.32 ± 0.04	3.30 ± 0.03	–
$Al(OH)_2Asp$	-1.74 ± 0.08	-2.32 ± 0.07	–
$Al_2(OH)Asp$	6.30 ± 0.04	–	–

sensitivity of this model to the choice of the hydrolytic model was examined by covariation of the stability constant of hydrolytic tridecamer, $(13, 0, -32)$, together with chosen speciation model. The calculation ended with slight change of the initial value of the stability constant of the tridecamer, from -106.50 to -106.92 and the stability constant of $(1, 1, -2)$ complex changed from -1.70 to -1.74 while other constants remained practically unchanged. This proves that the measured effects are from aluminum – aspartate complexation and not from aluminum hydrolysis only.

Reliability of the chosen model was tested by plotting the experimental and calculated titration curves (Fig. 2). Good coincidence between these curves confirms the reliability of the model. Our model is in good agreement with that derived by *Kiss et al.* [11]. The only difference between the two models is inclusion of the mixed dimmer, Al_2AspH_{-1} in our model. We previously found this species in aluminum – histidine solutions [17] and similar species, Al_2LH_{-2}, was found in Al – glycine, serine, threonine, and histidine systems [7], while the species Al_2LH_{-1} was found in aluminum – glutamate solutions [9, 18].

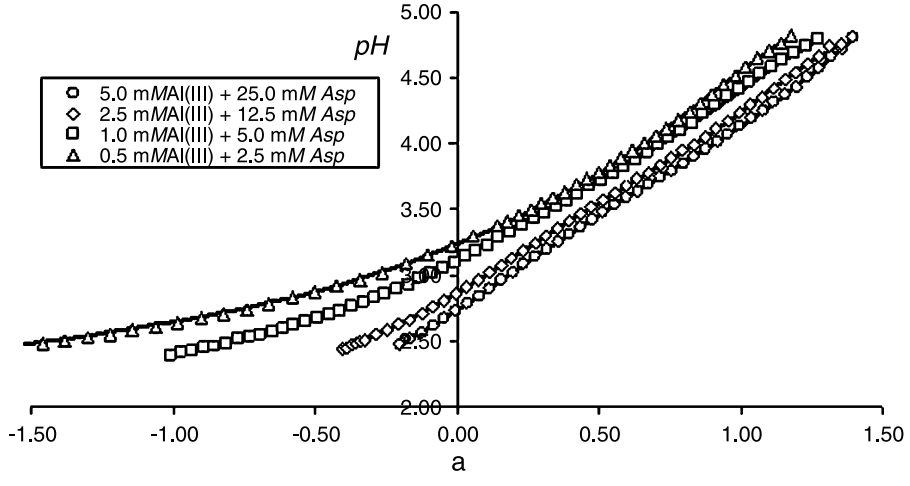

Fig. 2. Experimental and calculated titration curves in aluminum – aspartic acid systems; the titration parameter, **a**, is defined as $\mathbf{a} = (C_b V_b - C_{HCl} V_0)/C_{Asp} V_0$; concentration ratio of aspartate to aluminum is 5:1; $mM = \text{mmol/dm}^3$

The distribution diagrams at different ligand to metal concentration ratios are shown in Fig. 3a, b, and c.

It is seen from Fig. 3a–c that at $L/M = 5$, AlLH complex dominates and formation of hydrolytic Al_{13}-mer is fully suppressed. The dimer, Al_2LH_{-1} is formed in relatively low concentrations. At $L/M = 3$ the concentration of the dimer increases and Al_{13}-mer appears. At $L/M = 1$ hydrolysis is very pronounced, AlLH and AlL are formed in relatively low proportion while the concentration of the dimer, Al_2LH_{-1} rapidly increases. The Al_{13}-mer is formed in high concentrations at pH values higher than 4.2.

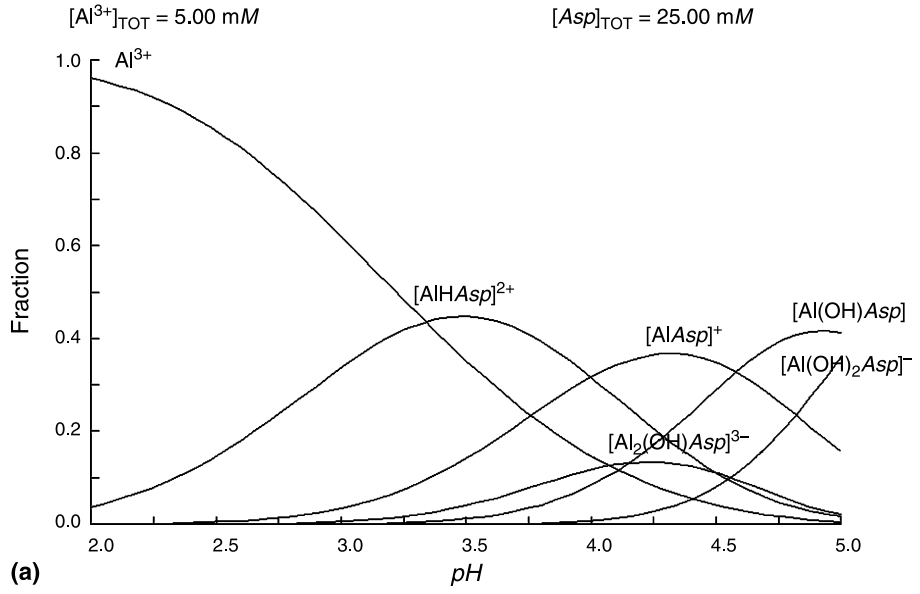

Fig. 3 (*continued*)

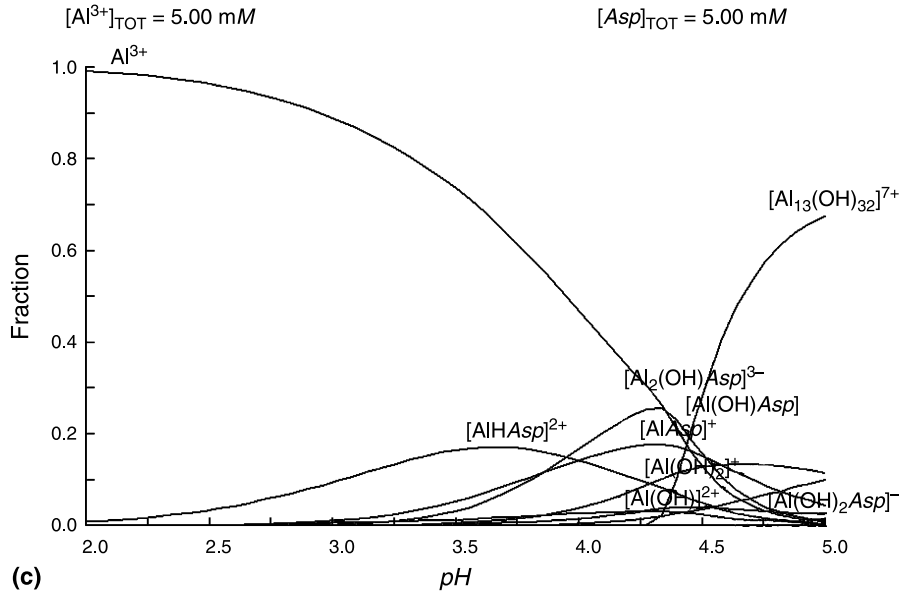

Fig. 3. Distribution diagrams of aluminum – aspartate species at different ligand to metal concentration ratios calculated using the program Medusa [19]; (a) $L/M = 5$; (b) $L/M = 3$; (c) $L/M = 1$

^{1}H NMR Spectra

Two series of solutions were prepared for recording the ^{1}H NMR spectra of aluminum – aspartate solutions. In a first series the M/L ratio was varied from 1:1 to 3:1 at $pH = 3.0$ and in a second series the pH was varied from 2.0 to 5.0 at $L/M = 2$ and $C_{Al} = 18.0\,\text{mmol/dm}^3$. The ^{1}H NMR spectrum of aspartic acid obtained at 25°C and at $pH = 2.5$ displayed two doublets (–CH_2–) centered at 2.951 and 2.984 ppm and two doublets (=CH–) centered at 4.022 and 4.060 ppm. Carboxyl and ammonium protons are normally not seen due to fast exchange. In the presence

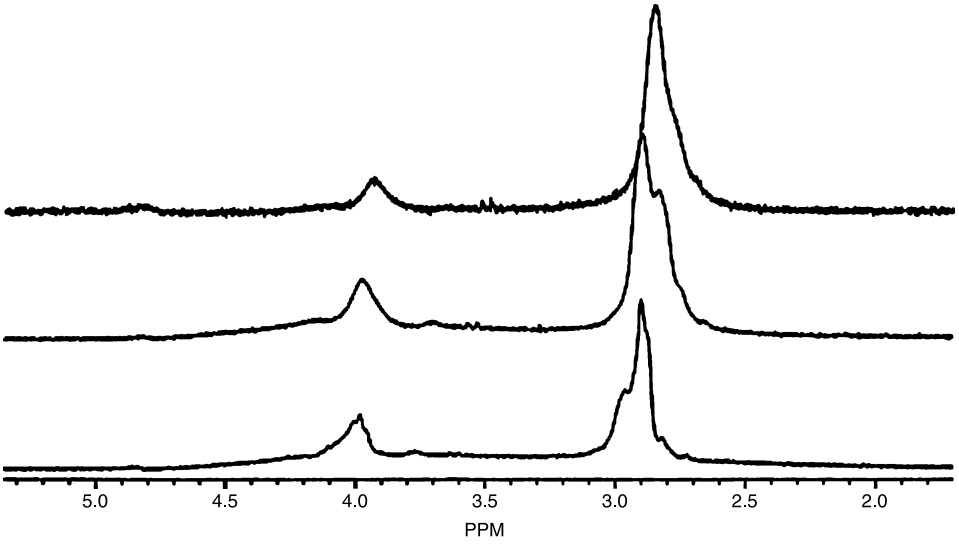

Fig. 4. ^{1}H NMR spectra of aluminum – aspartic acid solutions at different metal-to-ligand (M/L) concentration ratios at $pH = 3.0$; $M/L =$ (bottom upwards) 1, 2, and 3

of aluminum at $pH = 3.0$ and $M/L = 1$ shift of all signals toward lower δ and broadening of both signal patterns was observed (Fig. 4). Upon increasing M/L to 2 and 3 at the same pH value, further broadening of the signals with shift toward lower δ for about 0.6 ppm, occurs.

At $pH = 3.0$ and $L/M = 2$ broadening and high-field shifting (lower δ) of the signals is seen. The signal pattern for β-CH_2 was between 2.910–2.960 ppm and that for α-CH between 3.990–4.050 ppm. Increasing the pH to 4.0 leads to merging of the separate signals into broad rather featureless band. The observed spectral behavior may be explained by the significant formation of the dimeric species upon increasing the concentration ratio of aluminum to ligand and upon increasing the pH. At pH values higher than 3.5 the situation is rather complex since several species are formed in parallel *e.g.* MLH, ML, and M_2LH_{-1}.

^{13}C NMR Spectra

The ^{13}C spectrum of aspartic acid at $pH = 3.0$ (Fig. 5) displays four relatively sharp signals at 37.66 (β-CH_2), 53.75 (α-CH), 175.90 (γ-COOH), and 177.44 ppm (α-COOH).

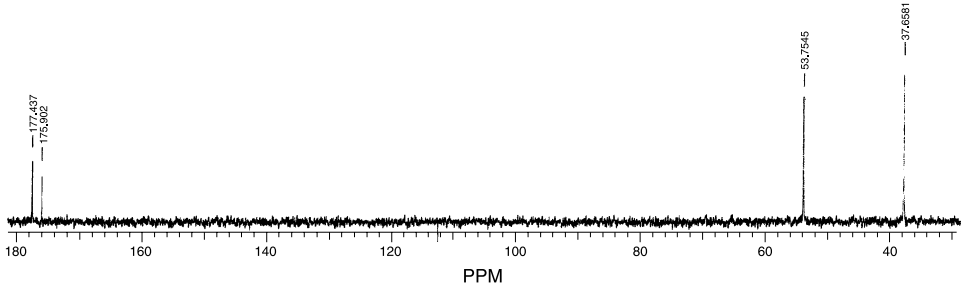

Fig. 5. ^{13}C NMR spectrum of aspartic acid at $pH = 3.0$

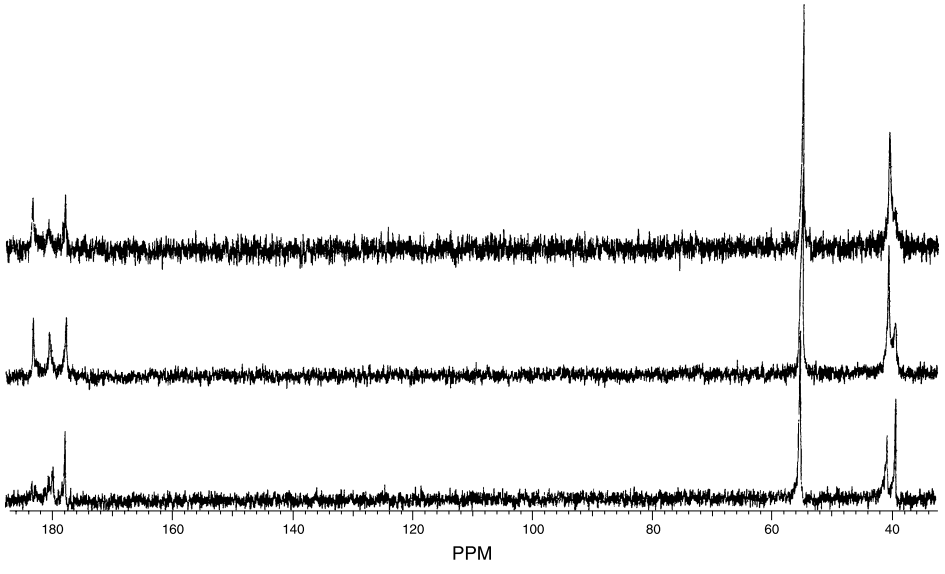

Fig. 6. NMR spectra of aluminum + aspartic acid solutions at different M/L ratios and $pH = 3.0$; $M/L = {}^{13}$C bottom upwards 1, 2, and 3; total aluminum concentration is 100 mmol/dm^3

Upon addition of aluminum ($C_{Asp} = 100\,\text{mmol/dm}^3$) at different M/L ratios ranging from 1:1 to 3:1 at $pH = 3.0$ the spectra undergo drastic changes (Fig. 6). New groups of signals belonging to coordinated aspartate appear in addition to signals belonging to free aspartic acid. The peaks which indicate coordinated aspartic acid at 39.8 ($-CH_2-$), 177.9, and 180.4 ppm (two carboxylates) are shifted to lower δ values compared to peaks of unbound aspartate. Upon increasing the M/L ratio signals form coordinated aspartate broaden.

If at $L/M = 1$ the pH is raised to 4.0 complex signal pattern is obtained (Fig. 7). All signals show high-field shift and additionally several signals belonging to coordinated aspartate appear. This is in accordance with potentiometric results which indicate formation of MLH, ML, and $M_2L\text{H}_{-1}$ in this pH region in significant amounts.

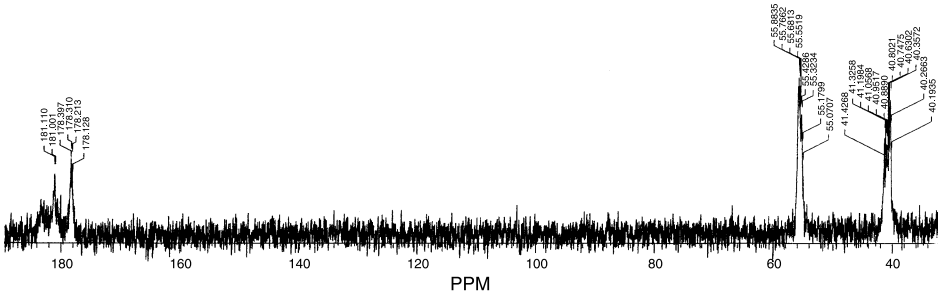

Fig. 7. ^{13}C NMR spectrum of aluminum + aspartic acid solution at $pH = 4.0$ and $L/M = 1$; total aluminum concentration is $100.0\,\text{mmol/dm}^3$

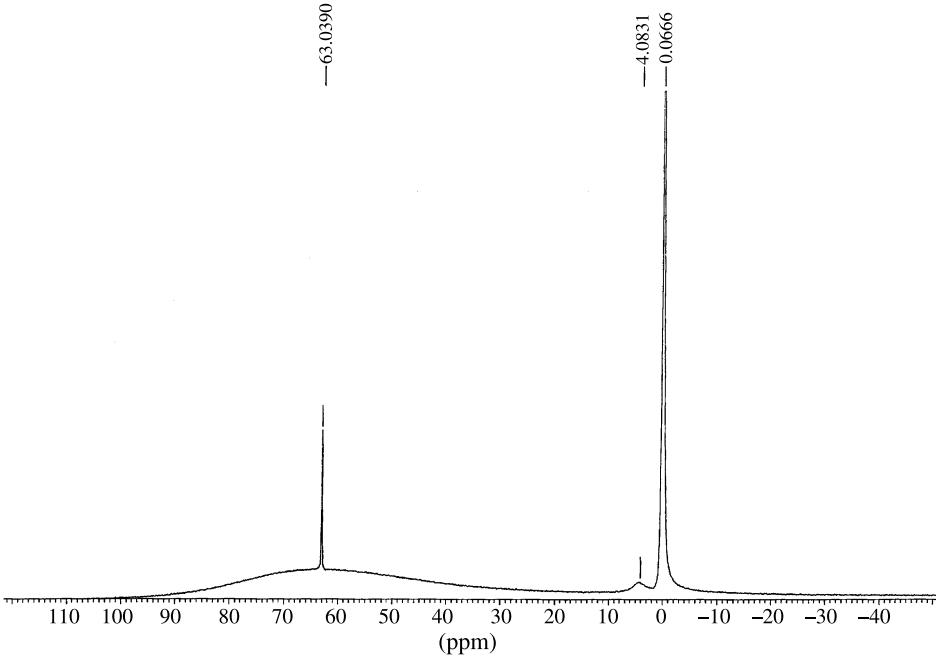

Fig. 8. ^{27}Al NMR spectrum of aluminum chloride solution at $pH = 3.0$ and total concentration of aluminum $100.0\,\text{mmol/dm}^3$

^{27}Al NMR Spectra

The ^{27}Al NMR spectra were taken of solutions in which the concentration of aluminum was 5.0 mmol/dm^3 and that of aspartic acid was 25.0 mmol/dm^3. The *pH* of solutions were 1.50, 3.80, and 4.50. First the spectra without the addition of the ligand were recorded using the solutions in which the concentration of aluminum was 50.0 mmol/dm^3 in *pH* interval from 1.80 to 5.50 (Fig. 8).

These spectra were taken 72 h after the preparation of the solutions. In acidic solutions (*pH* less than 3.0) only the peak at $\delta\sim0$ ppm was observed. At *pH* values between 3.0 and 4.0 the line at $\delta\sim0$ ppm broadens, with appearance of a tiny resonance at $\delta\sim0.8$ ppm, a small broad resonance at 4.08 ppm, and a sharp resonance at $\delta\sim63.04$ ppm (Fig. 8). According to literature data [20–23] resonance at $\delta\sim0$ ppm is assigned to $Al(H_2O)_6^{3+}$, broadening of this resonance upon slight increase of *pH* can be attributed to the formation of $Al(OH)(H_2O)_2^{2+}$ hydrolytic complex, while the resonance at 0.8 ppm and that at 4.3 ppm belong to oligomers most probably dimers, $Al_2(OH)_2^{4+}$, or $Al_2(OH)_4^{2+}$, and the trimer, $Al_3(OH)_4^{5+}$, respectively. The resonance at 63.04 ppm is due to tetrahedral aluminum of the Al_{13}-mer ''core''. Increase of the *pH* of solutions leads to the appearance of a rather broad peak at $\delta\sim4.3$ ppm and to a decrease of the intensity of the peak at 0 ppm. At *pH* values higher than 5.5 the peak at 4.3 ppm merges into the baseline and resonance at $\delta\sim0$ ppm disappears. The resonance at 63 ppm is observable up to

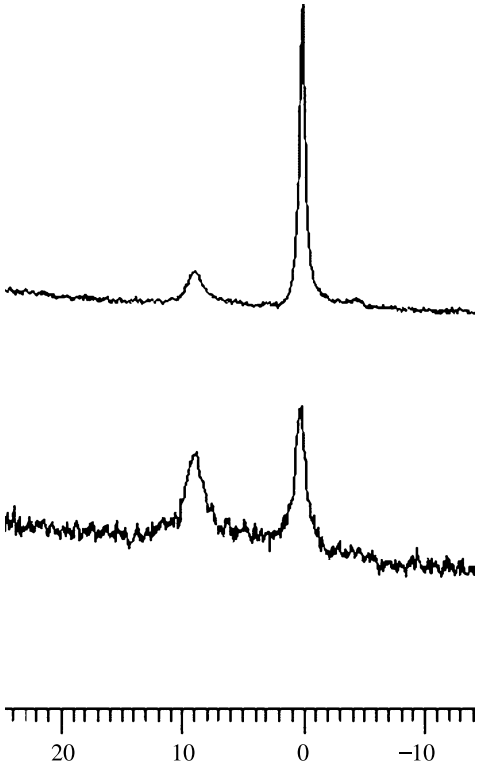

Fig. 9. ^{27}Al NMR spectra of aluminum + aspartic acid solutions at $pH = 3.80$ (upper spectrum) and $pH = 4.50$ (bottom spectrum) at total aluminium concentration 5.0 mmol/dm^3, $L/M = 5$)

pH about 5.80 and then disappears. The observed features of the spectra could be explained by the assumption that tridecamer and smaller oligomers act as precursors for the formation of $Al(OH)_3$ which finally precipitates and gives no signal in the spectrum [20]. To evaluate the complexation in aspartic acid + Al^{3+} solutions the prepared solutions were left to stand 72 h before measurements were made. Final check of the *pH* of solutions was done 30 min before recording the spectrum. The recorded spectra are shown in Fig. 9.

At $pH = 3.80$ the spectrum displays three resonances at $\delta \sim 0.0$, 4.2, and 9.80 ppm. The resonance at 9.80 ppm is near to expected value of $\delta \sim 10$ ppm when the amino acid acts as chelating ligand [24] and may be thus, assigned to the formation of binary complex between aluminum ion and aspartate. In this *pH* region the dominating complex is $Al(Asp)^{3+}$ and therefore, aspartate acts as in a fairly symmetrical environment. Bearing in mind that pK_a value of the γ-carboxyl group is about 4.0 it appears that γ-carboxylate is coordinated to aluminum in parallel with α-amino and carboxylate groups. Thus the complex is formed by tridentate binding of aspartate to aluminum.

Upon increasing the *pH*, the resonance at ~0 ppm broadens and decreases in intensity, the resonance at ~4.6 ppm merges into the baseline while the resonance at ~10 ppm increases in intensity and slightly broadens. At both examined *pH* values only a small resonance at ~63 ppm is seen meaning that the formation of Al_{13}-mer is a great deal suppressed.

Afore presented discussion of the multinuclear NMR spectra leads to conclusion that in Al(H*Asp*) complex aspartate acts as a bidentate ligand with a probable formation of five-membered ring by α-carboxylate and amino groups. Since however, the most pronounced spectral changes are observed on β-methyl group it means that this group is situated close to the ring plane so that both hydrogens and carbon as well undergo the influence of coordinated groups while such influence on methylene group is much less pronounced (Scheme 1). This structure however is not preferable to the one with a seven-membered ring and two COO^- donors. Though seven-membered rings are usually less stable than five- or six-membered rings from sterical reasons its formation may be, in case of symmetrical structures, very probable. The protonated complex, Al(H*Asp*), is fairly stable (log *K*: $(Al^{3+} + HAsp^- \rightleftharpoons Al(HAsp)^{2+}$, 2.19) so that bidentate behavior of aspartate is certain. It seems that both isomers, with five-membered ring and

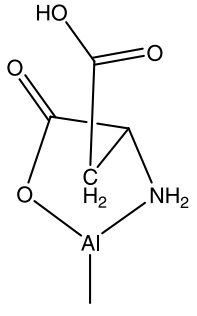

Scheme 1. Possible structure of $Al(HAsp)^{2+}$ complex in solution; coordinated water molecules are omitted from the coordination sphere

seven-membered ring coexist in equilibrium. Structural features of Al(*Asp*) complex cannot be easily derived from ^{1}H and ^{13}C NMR spectra because in the *pH* region in which its concentration is maximal, other complexes form in parallel, especially the dimer so that spectral patterns reflect rather combined complexation effects. In ^{27}Al NMR spectrum the position of the resonance at $\sim$10 ppm and its symmetrical form indicate rather slow exchange time on NMR scale. It means that the ligand is firmly bound in the complex of a higher symmetry. Such situation may arise either in tridentately bound ligand or in bidentately bound ligand in which case the formula of the complex should be. Al(OH)H*Asp* with OH group bonded directly to aluminum. Formation of bidentate hydroxo isomer is not very probable since other amino acids do not form such isomer and aspartic acid with other metal ions forms tridentate complexes [12, 20]. Thus, bearing in mind the relatively high value of the stability constant (Table 3) for the $Al(Asp)^{2+}$ complex, it may be inferred that aspartate is bound tridentately to aluminum.

Synthesis of Al – *Asp* Complex

Upon addition of aspartic acid to freshly precipitated $Al(OH)_3$ the precipitate readily dissolves yielding clear solution. Thus, we prepared the Al – *Asp* complex in the following way:

To 10 cm^3 of acidified solution of $AlCl_3$ (0.5 mol/dm^3), heated to 40°C, the diluted (1:1) ammonia solution was added drop-wise. The precipitate was transferred to a round bottom flask and thoroughly washed with distilled water. To this precipitate 10 mmol of recrystallized solid aspartic acid were added, the *pH* was adjusted to 3.5, and the mixture was heated to 40°C. The reaction mixture was refluxed for about 12 h on a rotating head. The content was then transferred to a crystallization dish, cooled to room temperature, and gently evaporated by stream of air until minimum volume was reached. The solution was then cooled slightly below room temperature during which procedure the white gelatinous substance with silvery shine, separated. Upon air drying for three days, white microcrystalline substance was obtained. The substance is moderately soluble in water, the *pH* of a 5 $mmol/dm^3$ solution is 4.0. This substance was characterized by elemental analysis, IR, and NMR spectra. Elemental analysis (Table 4) unambiguously shows the presence of chloride and crystal water in the separated complex. Amongst different possibilities the best agreement between found and calculated data was for the $[Al(Asp)]Cl \cdot 3H_2O$ complex.

In Fig. 10, IR spectra of pure aspartic acid (a) and Al – *Asp* complex (b) are shown. The spectrum of the complex differs from that of the pure acid in the region of NH_2 and carboxylate –C=O vibrations. Band shapes and positions are significantly changed as evidenced from Fig. 10. This confirms complex formation. In the

Table 4. Elemental analysis of Al – *Asp* complex; calculated values for $[Al(Asp)]Cl \cdot 3H_2O$

	C	H	N	Cl
Calcd.	19.4	4.5	5.7	14.3
Found	19.7	5.8	5.9	15.0

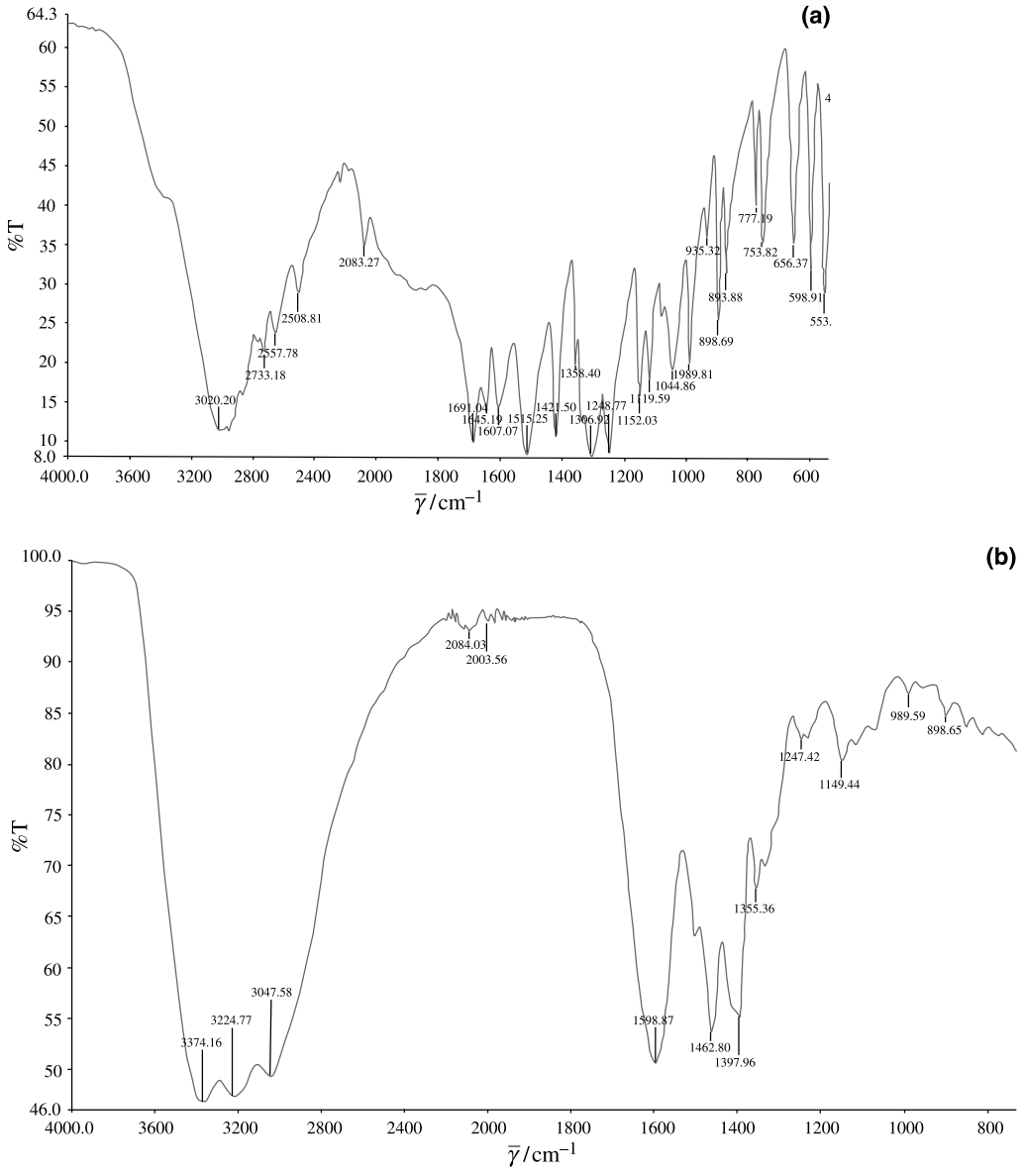

Fig. 10. (a) Infrared spectrum of aspartic acid (hydrochloride); (b) infrared spectrum of Al – aspartic acid complex

same time in the spectrum of the complex, the vibration belonging to coordinated NH_2 is found at 3374 and 3224 cm^{-1}. At 1598 cm^{-1} the vibration of $–COO^-$ is seen. No vibrations of –COOH are seen in the spectrum of the complex (both carboxyls are deprotonated) [25]. It can be inferred that in solid state tridentate chelate is formed. Its structure may be similar to that of magnesium – *L*-aspartate complex [26] with five- and six-membered rings in equatorial position. The ^{13}C spectrum of the substance dissolved in D_2O shows the chemical shifts δ $(COO^-) = 180.6,\ 179.1$ ppm, δ $(CH_2) = 55.9$ ppm (center of multiplet), and δ

(CH) = 40.2 ppm (center of multiplet). This spectrum roughly corresponds to the one observed in solution at *pH* values lower than 4.0.

Materials and Methods

Chemicals and Solution

The aluminum chloride stock solution was obtained by dissolving $AlCl_3 \cdot 6H_2O$, *pa*, Merck (Darmstadt, FRG), in doubly distilled water. The appropriate amount of 0.1 mol/dm^3 of HCl was added to prevent initial hydrolysis of aluminum. The aluminum content in solution was determined gravimetrically by precipitation with ammonia or 8-hydroxychinoline. Both methods gave the same results within 0.3%. The concentration of the free acid was determined potentiometrically with standard NaOH using the *Gran* plot. The metal and proton content in the solution was periodically checked before each series of experiments. *L*-Aspartic acid, *pa*, Merck, was dissolved in doubly distilled water and assayed potentiometrically. The sodium hydroxide solution was prepared from a concentrated volumetric solution, *pa*, Merck, by diluting with freshly boiled doubly distilled water, cooled under constant flow of purified nitrogen. The alkali concentration was checked by titration against potassium hydrogen phthalate. The hydrochloric acid solutions were prepared from HCl, "Suprapure", Merck and standardized against tris(hydroxymethyl)aminomethane.

Instruments and Procedure

All *pH* measurements were made by using Beckman model 4500 digital *pH*/mV-meter equipped with Beckman combined electrode. The electrode was calibrated with standard Beckman *pH* 4.01 and 7.00 buffers. The potentiometric titrations were performed in a double mantled, thermostated vessel at 298.0 ± 0.1 K and at constant ionic strength (0.1 mol/dm^3 LiCl) under nitrogen atmosphere. The acidified solution of aluminum + *L*-aspartic acid was titrated with the standard solution of sodium hydroxide. Before commencing the titrations the acidified solutions were allowed to stand for 24 h. To reduce the concentration of the hydrogen ion in the titrated solutions, the titrant was added stepwise in small aliquots (0.005–0.01 cm^3). Titrant was delivered form the Metrohm Dosimat model 665 (Herissau, Swiss) under energetic stirring of the solution. The potential (or *pH*) was monitored after each addition of a titrant. The readings were taken every 2 min until steady values to ± 0.1 V (±0.002 *pH* units) were obtained. Usually stable potential readings were obtained in 5–10 min after addition of the titrant at the beginning of the titration ($pH < 3$) and in 15–20 min at *pH* values higher than 3. The potential at some titration points was even monitored for 60 min to make sure that the solution did not become supersaturated with respect to polynuclears or $Al(OH)_3$. All titrations were carried in duplicate. The agreement between duplicate titration was better than 1%. The electrode was calibrated to hydrogen ion concentration using the previously described method [7, 17]. The electrode calibration was made by the titration of a mixture of HCl and tris(hydroxymethyl)aminomethane by NaOH before each experiment. The water autoprotolysis constant was determined as $pK_w = 13.72 \pm 0.02$. The species formed in the systems were characterized by the general equilibrium (Eq. (6)) and the corresponding constants are given by Eq. (7) where *Asp* is the non-protonated molecule of the ligand.

$$p\mathrm{Al} + qAsp + rH \rightleftharpoons \mathrm{Al}_p(Asp)_q\mathrm{H}_r \tag{6}$$

$$\beta_{p,q,r} = \frac{[\mathrm{Al}_p(Asp)_q\mathrm{H}_r]}{[\mathrm{Al}]^p[Asp]^q[\mathrm{H}]^r} \tag{7}$$

Fully protonated aspartate is denoted as H_3Asp^+. The concentration stability constants of complexes, $\beta_{p,q,r}$, were calculated with the aid of the computer program Hyperquad [14, 15]. The *pH*-metric data between $pH = 2.5$ and 5.0 were used for evaluation. To derive the reliable complexation model very accurate data on pure hydrolysis of aluminum are needed. Namely, the hydrated aluminium(III) ion is very prone to hydrolysis in water solutions. The extent of hydrolysis, the identity and stability of

hydrolytic species formed in solution, depend upon many factors such as the nature and concentration of supporting ionic medium, the nature and concentration of the base used to force the hydrolysis, ageing time, and the presence of other substances that may interact with either aluminum ion or water molecules or both [1]. Pronounced hydrolysis of aluminum ion could considerably obscure weak complexation in solution [1]. Furthermore, polynuclear hydrolytic species whose rate of formation is quite slow so that they may persist in solution for long period of time as metastable species even if the actual *pH* of the solution corresponds to the conditions where they are no longer the most stable species, make the identification of complexes very difficult. The solution could also become supersaturated with respect to one or more polynuclears or solid hydrated oxide of aluminum which further complicates the complexation. To make sure that the measured *pH* effects are due to complexation and not to pure hydrolysis of aluminum, very reliable data on aluminum hydrolysis are necessary, relatively high concentration ratios of ligand to aluminum should be used, and several experimental techniques must be combined. The diversity of factors which influence the hydrolysis creates the situation where there is no unique model for aluminum ion hydrolysis. In the milimolar range of the total aluminum concentration in solution and the *pH* interval from *ca.* 3 to 5 the common consensus is that $Al(OH)^{2+}$, the oligomer, and $[Al_{13}O_4(OH)_{24}(H_2O)_{12}]^{7+}$ (to which we will refer as Al_{13}-mer) are the main constituents of the solution [27]. Essentially the same model was determined in our previous works, in 0.1 mol/dm^3 LiCl ionic medium at 298 K. Thus, based on the previously reported hydrolytic models [1] for the analysis of the titration curves the hydroxo species AlH_{-1} (-5.27), AlH_{-2} (-9.53), AlH_{-3}(aq) (-14.68), AlH_{-4} (-23.1), Al_3H_{-4} (-13.81), and $Al_{13}H_{-32}$ (-106.5) were taken into account [17].

The ^{27}Al NMR spectra were recorded at 104.26 MHz on a Bruker MSL 400 spectrometer. Samples were recorded in 10 mm tubes, with $AlCl_3$ in 6 mol/dm^3 HCl, as an external standard. D_2O was added in each sample for a lock. The FT-NMR measurement conditions were as follows: pulse width 7 μs, flip angle 45°, acquisition time 98.3 ms, spectral width 20833 Hz, number of transients 200–500, pulse repetition time 1 s, number of data points 4 k, digital resolution 10.17 Hz/point. The ^1H and ^{13}C NMR spectra were recorded on a Varian Gemini 200 spectrometer using NMR tubes 5 mm in diameter and D_2O as solvent. For ^1H NMR spectra the D_2O solution of DSS was used as an external standard. FT operating parameters were: proton frequency 199.975 MHz, spectral width 2500 Hz, acquisition time 2.662 s, relaxation delay 1.0 s, pulse width 45°, no of repetition 16, FT size, 16 K. For ^{13}C spectra *TMS* was used as in internal standard with operational parameters: carbon frequency 50.286 MHz, spectral width 14,992.5 Hz, acquisition time 1.0 s, pulse width 32°, no of repetitions 54272, FT size 32 K. The *pD* of the solutions was adjusted by the addition of either DCl or KOD. The *pD* was calculated from the measured *pH* through the equation: $pD = pH + 0.4$.

Acknowledgement

Financial support from the Ministry of Science and Technology of the Republic of Serbia is gratefully acknowledged.

References

[1] Special recent issues of the journals devoted to aluminum toxicity and chemistry: J Inorg Biochem (2003) **97**: Iss. 1; J Inorg Biochem (2001) **87**: Iss. 1-2; J Inorg Biochem (1992) **76**: Iss. 2; Coord Chem Rev (2002) **228**: Iss. 2; Coord Chem Rev (1996) **149**

[2] Nayak P (2002) Environ Res A **89**: 101

[3] Gitelman HJ (ed) (1989) Aluminum and Health. A Critical Review, M. Dekker, New York; Van Landeghem FG, De Broe EM, D'Haese CP (1998) Clinical Biochem **31**: 385

[4] Martell A, Hancock DR, Smith MR, Motekaitis JR (1996) Coord Chem Rev **149**: 311; Martell EA, Motekaitis JR, Smith MR (1990) Polyhedron **9**: 171

[5] Williams JPR (1966) Coord Chem Rev **149**: 1; Alfrey CA (1995) Toxicity of Detrimental Metal Ions. Aluminum. In: Berthon G (ed) Handbook of Metal-Ligand Interactions in Biological Fluids, vol 2. Bioinorganic Medicine, M. Dekker, New York, pp 735–740
[6] Kiss T, Jakusch T, Kilyen M, Kiss E, Lakatos A (2000) Polyhedron **19**: 2389; Orvig C (1993) The Aqueous Coordination Chemistry of Aluminum. In: Robinson HG (ed) Coordination Chemistry of Aluminum, VCH, Weinheim, pp 85–121
[7] Dayde S, Champmartin D, Rubini P, Berthon G (2002) Inorg Chim Acta **339**: 513
[8] Kiss E, Lakatos E, Banyai I, Kiss T (1998) J Inorg Biochem **69**: 145
[9] Dayde S, Brumas V, Champmartin D, Rubini P, Berthon G (2003) J Inorg Biochem **17**: 104
[10] Yang X, Tang Y, Bi S, Yang G, Hu J (2003) Anal Sci **19**: 133
[11] Kiss T, Sovago I, Toth I, Lakatos A, Bertani P, Tapparo A, Bombi G, Bruce Martin R (1997) JCS Dalton Trans 1967
[12] Laurie S (1987) Amino Acids, Peptides and Proteins. In: Wilkinson G, Gillard DR, McCleverty AJ (Eds) Coordination Chemistry, Pergamon Press, Oxford pp 739–776; Jakubke DH, Jeshkeit H (1982) Aminosauren, Peptide, Proteine, Akademie Verlag, Berlin; Van der Voet BG (1992) Aluminum in Biology and Medicine, Ciba Foundation Symposium 169. Wiley, Chichester, pp 109–122
[13] Charlet Ph, Deloume PJ, Duc G, Thomas-David G (1984) Bull Soc Chim Fr **7–8**: 222
[14] Gans P, Sabatini A, Vacca A (1996) Talanta **43**: 1739
[15] Gans P, Sabatini A, Vacca A (1985) J Chem Soc Dalton Trans 1195
[16] Dayde S (1990) Etude des equilibres de complexation et speciation simulee de la fraction ultrafiltrable de l'aluminium dans le plasma sanguine et la fluide gastro-intestinal. Implications pour la toxicite de l'aluminium. These de Doctorat de l'Universite Paul Sabatier, Toulouse, France
[17] Djurdjevic P, Jelic R, Dzajevic D, Cvijovic M (2002) Metal Based Drugs **8**: 235
[18] Djurdjevic P, Jelic R (1998) Main Group Metal Chem **21**: 331
[19] Puigdomenech I (1983) Input, Sed and Predom: Computer programs drawing equilibrium diagrams, Technical report TRITA-OOK-3010. Royal Institute of Technology, Dept Inorg Chem Stockholm
[20] Akitt WJ (1989) Prog Nucl Mag Res Spectr **21**: 1
[21] Tossell AJ (2001) Geochim Cosmochim Acta **65**: 2549; Bertsch PM, Parker RD (1996) Aqueous Polynuclear Aluminum Species. In: Sposito G (ed) The Environmental Chemistry of Aluminum, Lewis Publ., Boca Raton, 2nd Edition, pp 117–168
[22] Perry K, Shafran L (2001) J Inorg Biochem **87**: 115
[23] Ohman OL, Sjoberg S (1996) Coord Chem Rev **149**: 33
[24] Karweer BS, Pillai PB, Iyer KR (1990) Magnetic Res Chem **28**: 922; Karweer BS, Pillai PB, Iyer KR, Indian J Chem **30A**: 1064
[25] Bellamy JL (1975) The Infrared Spectra of Complex Molecules, Vol 1, Chapman and Hall, London, pp 266, 273; Barth A (2000) Prog Biophys Mol Biol **74**: 141
[26] Schmidbaur H, Bach I, Wilkinson LD, Muller G (1989) Chem Ber **122**: 1445; Schmidbaur H, Muller G, Riede J, Manninger G, Helbig J (1986) Angew Chem Int Ed **25**: 1013
[27] Singhal A, Keefer DK (1994) J Mater Res **9**: 1973; Ohman OL, Sjoberg S, Ingri N (1983) Acta Chem Scand Ser A **37**: 561; Hedlund T, Sjoberg S, Ohman OL (1987) Acta Chem Scand Ser A **41**: 197